

HORIZON EUROPE PROGRAMME
HORIZON-JTI-CLEANH2-2024

GA No. 101192342

**Direct seawater electrolysis technology for
distributed hydrogen production**



SWEETHY - Deliverable report

D5.1 – Corrosion of uncoated BPP and PTL materials



Deliverable No.	D5.1.	
Related WP	WP5	
Deliverable Title	Corrosion of uncoated BPP and PTL materials	
Deliverable Date		
Deliverable Type	Report	
Dissemination level	Public (PU)	
Author(s)	Sourav Bhowmick (IC), Michel Prestat (IC), Andrea Valencia (CIDETEC), Francisco Alcaide (CIDETEC)	2026-05-13
Reviewed by	Daniel Garcia-Sanchez (DLR), Marco Rivera-Gil (DLR)	2026-05-20
Approved by	Olesia Danyliv (RISE)	2026-06-05
Status	Final	2026-06-05



Project Summary

SWEETHY will develop an advanced technology for direct seawater electrolysis that will be able to produce H₂ and O₂ under intermittent conditions, accounting for the coupling to renewable power sources (especially wind, PV). The electrolyser will be based on an anion exchange membrane (AEM) operating in natural or alkaline seawater, and the SWEETHY technology will be developed along three dimensions:

- a) Materials optimisation. To meet the specific requirement of the seawater environment, the project will focus on corrosion resistance and selective PGM-free electrocatalysts for hydrogen and oxygen evolution reactions, on AEM with high selectivity for transporting hydroxide anions and anti-fouling properties, as well as on novel anti-corrosion coatings for bipolar plates and porous transport layers prepared by plasma spraying and electrodeposition.
- b) Electrolyser stack prototyping. The project will exploit a novel stack architecture, which uses hydraulic cell compression to host the advanced materials and to produce H₂ at high pressure. The beneficial functions of the targeted unique stack are related to scalability and maintainability that will be tremendously improved in comparison to conventional AEMWE stacks.
- c) Sustainability analysis. The project will conduct studies (life-cycle assessment (LCA), techno-economic analysis (TEA)) to evaluate the circularity of the electrolyser system and its integration into renewable-power systems and to explore an efficient by-product utilisation way through industrial symbioses. These studies will feed back to materials optimisation and stack development. Complementing LCA, social LCA, and techno-economic analyses/optimisation by qualitative work ensures both environmental, economic, and social sustainability.

Combining these three dimensions, SWEETHY will utilise Mediterranean seawater from the coast of Messina, Italy, to test its electrolyser with the goal withstand more than 2000 h of operation to produce 20 g_{H2}/h with a degradation rate lower than 1%/100h. In addition, SWEETHY will demonstrate how the operation of the electrolyser can ensure an optimised revenue concerning by-products and grid services.



Public Deliverable Summary

Deliverable 5.1 reports the assessment of corrosion behavior of potential bipolar plates (BPP) and porous transport layers (PTL) materials without protective coatings for AEM-based direct seawater electrolysis.

In this work, the corrosion of flat nickel, titanium, stainless steel (316L), and nickel-based alloys (Monel 400, Inconel 600, Inconel 625, C22) plates was investigated in KOH and in alkaline artificial seawater (ASW) at pH ~ 14 at 50°C for 2 days and 7 days under potentiostatic anodic and cathodic polarization. The surface state of the samples before and after polarization was compared using scanning electron microscopy (SEM), energy-dispersive X-ray spectroscopy (EDX), Raman microscopy, and profilometry to evaluate corrosion damage. The activities were mainly focused on the anodic polarization that leads to the most significant corrosion damage.

The main results are:

- Three main kinds of degradation were observed: pitting corrosion (seen as severe degradation) and formation of oxide/hydroxide layers (seen as mild degradation), whose thickness depends on the testing conditions (potential, electrolyte composition, and time), and absence of degradation (sometimes associated with surface discoloration but without significant oxide/hydroxide development concentration on the surface (below EDX detection limit)).
- In KOH electrolyte (in the absence of chlorides) under anodic polarization: Pure nickel and Ni-based alloys (Monel 400, Inconel 600, Inconel 625, C22) are stable but develop an oxide/hydroxide layer whose thickness depends on the applied potential and duration. Titanium and 316L are not stable for long durations due to metal dissolution and leaching, respectively.
- In ASW (in the presence of chlorides) under anodic polarization: Nickel, titanium, 316L, as well as molybdenum-free Monel 400 and Inconel 600 heavily corrode (pitting corrosion) while the nickel-based alloys containing molybdenum and a higher amount of chromium (Inconel 625, C22) develop an oxide/hydroxide layer whose thickness increases with time and with increasingly anodic potentials. The thickest coatings exhibit cracks and, in some cases, fragments of them peel off the surface.
- In ASW (in the presence of chlorides) under cathodic polarization: Titanium is stable (no pitting or metal dissolution) but develops an oxide/hydroxide layer on the surface, whose thickness depends on the applied potential and duration. 316L and Ni-based alloys (Monel 400, Inconel 600, Inconel 625) are stable for long durations with no formation of oxide/hydroxide on the surface.



Contents

1	Introduction	10
2	Experimental	10
2.1	Methods	10
	<i>Substrate Materials</i>	10
	<i>Electrolytes</i>	10
	<i>Electrochemical characterization of substrates</i>	11
	<i>Physicochemical characterization of substrates</i>	11
2.2	Anodic Polarization	12
2.2.1	Nickel (Ni).....	12
	<i>In 1M KOH (pH ~ 14)</i>	12
	<i>In Alkaline Artificial Seawater (pH ~ 14)</i>	12
2.2.2	Titanium (Ti)	13
	<i>In 1M KOH (pH ~ 14)</i>	13
	<i>In Alkaline Artificial Seawater (pH ~14)</i>	15
2.2.3	Stainless Steel (316L).....	17
	<i>In 1M KOH (pH ~ 14)</i>	17
	<i>In Alkaline Artificial Seawater (pH ~ 14)</i>	18
2.2.4	Monel 400.....	19
	<i>In 1M KOH + 0.6 M NaCl solution (pH ~ 14)</i>	19
2.2.5	Inconel 600	19
	<i>In 1M KOH (pH ~ 14)</i>	19
	<i>In Alkaline Artificial Seawater (pH ~ 14)</i>	21
2.2.6	Inconel 625	21
	<i>In 1M KOH (pH ~ 14)</i>	21
	<i>In Alkaline Artificial Seawater (pH ~ 14)</i>	22
2.2.7	C22 Alloy	23
	<i>In 1M KOH (pH ~ 14)</i>	23
	<i>In Alkaline Artificial Seawater (pH ~ 14)</i>	24
2.3	Cathodic Polarizations	26
2.3.1	Titanium (Ti)	26
	<i>In Alkaline Artificial Seawater (pH ~ 14)</i>	26



2.3.2	Stainless Steel (316L).....	27
	<i>In Alkaline Artificial Seawater (pH ~ 14)</i>	27
2.3.3	Monel 400.....	28
	<i>In Alkaline Artificial Seawater (pH ~ 14)</i>	28
2.3.4	Inconel 600	29
	<i>In Alkaline Artificial Seawater (pH ~ 14)</i>	29
2.3.5	Inconel 625	29
	<i>In Alkaline Artificial Seawater (pH ~ 14)</i>	29
3	Contribution to Project Specific Objectives	30
4	Contribution to major project exploitable result	30
5	Conclusions and Recommendations.....	31
6	Acknowledgement.....	34



List of Figures

Figure 1: (a) Photograph of Ni substrate polarized for 2 days at 1.6V at 50 °C in 1M KOH. The exposed surface is the round-shaped area in the centre. The rest of the sample was not exposed to the electrolyte. SEM images of the Ni substrate in (b) the pristine state, and (c) after polarization.	12
Figure 2: (a) Photograph of Ni substrate polarized in alkaline ASW for 45 mins at 1.6V at 50 °C. The exposed surface is the round-shaped area in the centre (barely visible in this picture). The rest of the sample was not exposed to the electrolyte. (b) The electrolyte solution after polarization. SEM images of the Ni substrate in (b) the pristine state, and (c) after polarization.	13
Figure 3: (a-e) Polarization of Ti substrate at 1.6V at 50 °C in 1M KOH. Photographs of the Ti substrate polarized for (a) 2 days and (b) 7 days. The exposed surface is the round-shaped area in the centre. SEM images in (c) pristine state, (d) after polarization for 2 days, and (e) after polarization for 7 days.....	14
Figure 4: Raman spectra of Ti substrate polarized in 1M KOH at 2.2V at 50 °C for 7 days.....	15
Figure 5: (a-e) Polarization for 2days at 50 °C in alkaline ASW. Photographs of the Ti substrate polarized at (a) 1.6V and (b) 2.2V. The exposed surface is the round-shaped area in the centre. SEM images in (c) pristine state, (d) after polarization at 1.6V, and (e) after polarization at 2.2V.....	15
Figure 6: Raman spectra of Ti substrates polarized in alkaline artificial seawater at 50 °C for 7 days at an applied potential of (a) 1.6V and (b) 2.2V.....	16
Figure 7: Profilometry line scan along the diameter of the exposed surface area for the Ti substrates polarized for 7 days at 2.2V in (a) alkaline ASW and (b) 1M KOH.....	17
Figure 8: (a) Photograph of 316L substrate polarized for 7 days at 1.6V at 50 °C in 1M KOH. The exposed surface is the round-shaped area in the centre. The white marks along the side of the samples are remnants of the silicon gasket. SEM images of 316L substrate in (b) pristine state and (c) after polarization. (d) Photograph of the “yellow-brownish” electrolyte after polarization.	18
Figure 9: (a) Photograph of 316L substrate polarized for 2 days in alkaline artificial seawater at 1.6V at 50 °C. The exposed surface is the round-shaped area in the centre. (b) Photograph of the reddish electrolyte after polarization. SEM images of 316L substrate in (c) pristine condition and (d & e) after polarization.....	18
Figure 10: Photographs of Monel 400 substrates polarized at 50 °C for 2 days at an applied potential of (a) 1.7V and (b) 1.9V. The exposed surface is the round-shaped area in the centre.....	19
Figure 11: (a-c) Polarization at 1.8V at 50 °C in 1M KOH. (a) Photograph of Inconel 600 substrate polarized for 2 days. The exposed surface is the round-shaped area in the centre. SEM images of (b) pristine state, and (c) after polarization.	20
Figure 12: Photographs of Inconel 600 substrates polarized at 50 °C in alkaline artificial seawater for 2 days at (a) 1.8V, (b) 2V, and (c) 2.2V. The exposed surface is the round-shaped area in the centre.	21
Figure 13: (a-c) Polarization at 1.8V at 50 °C in 1M KOH. (a) Photograph of Inconel 625 substrate polarized for 2 days. The exposed surface is the round-shaped area in the centre. SEM images of (b) pristine Inconel 625 and (c) after polarization.	22
Figure 14: (a-c) Polarization at 1.8V at 50 °C in alkaline ASW. (a) Photograph of Inconel 625 substrate polarized for 2 days. The exposed surface is the round-shaped area in the centre. SEM images of (b) pristine Inconel 625 and (c) after polarization.	23



Figure 15: (a) Photograph of C22 substrate polarized in 1M KOH for 7 days at 1.6V at 50 °C. The exposed surface is the round-shaped area in the centre. SEM images in (b) the pristine state, and (c) after polarization.	24
Figure 16: (a-c) Polarization at 1.6V at 50 °C in alkaline ASW. (a) Photograph of C22 substrate polarized for 7 days. The exposed surface is the round-shaped area in the centre. SEM images of C22 in (b) pristine state, (c) after polarization.	25
Figure 17: Profilometry line scan along the diameter of the exposed surface area for the C22 substrates polarized for 7 days in alkaline ASW at (a) 1.8V and (b) 2V. The large noise at both ends of the line scan (a) is due to gasket pieces sticking to the substrate after cell dismantling.	26
Figure 18: Photographs of Ti substrates polarized in alkaline ASW at 50 °C for 7 days at a potential of (a) -0.3V and (b) -0.2V. The exposed surface is the round-shaped area in the centre. SEM images of Ti substrates in (c) pristine state, and after 7 days of polarization at (d) -0.3V and (e) -0.2V.	27
Figure 19: Photographs of 316L substrates polarized in alkaline ASW at 50 °C for 7 days at (a) -0.3V and (b) -0.2V. The exposed surface is the round-shaped area in the centre. SEM images of 316L substrates in (c) the pristine state and after 7 days of polarization at (d) -0.3V and (e) -0.2V.	27
Figure 20: (a) Photograph of Monel 400 substrate polarized in alkaline ASW for 2 days at an applied potential of -0.3V. The exposed surface is the round-shaped area in the centre. The SEM images of (b) the pristine Monel 400, and (c) after polarization.	28
Figure 21: (a) Photograph of Inconel 600 substrate polarized in alkaline ASW for 2 days at an applied potential of -0.3V. The exposed surface is the round-shaped area in the centre. SEM images of (b) the pristine Inconel 600 and (c) after polarization.	29
Figure 22: (a) Photograph of polarized Inconel 625 substrate in alkaline ASW for 2 days at an applied potential of -0.3V. The exposed surface is the round-shaped area in the centre. The SEM images of the (b) pristine state, and (c) after polarization.	30
Figure 23: (a) Sketch of the two types of degradation of uncoated substrates in the present study and (b) their possible consequences on the durability of a subsequently applied coating.	32

List of Tables

Table 1: Elemental composition of the different alloys (in wt%)	10
Table 2: Chemical composition of artificial seawater (mixed salts in 0.8L DI water).....	11
Table 3: Elemental analysis (SEM-EDX) of Ni substrate polarized in 1M KOH at 1.6V at 50 °C for 2 days.....	12
Table 4: Elemental analysis (SEM-EDX) of Ti substrate polarized in 1M KOH at 1.6V and 2.2V at 50 °C for 2 and 7 days.....	14
Table 5: Elemental analysis (SEM-EDX) of Ti substrate polarized in alkaline artificial seawater polarized for 2days and 7 days at an applied potential of 1.6V and 2.2V	16
Table 6: Interfacial contact resistance (ICR) values of Ti substrates polarized at 1.6V and 2.2V for 2 and 7 days.....	17
Table 7: Elemental analysis using SEM-EDX of 316L substrate polarized in 1M KOH at 1.6V at 50 °C for 7 days.....	18
Table 8: Elemental analysis (SEM-EDX) of Inconel 600 substrate polarized in 1M KOH for 2 days at an applied potential of 1.8V, 2V, and 2.2V.....	20
Table 9: Elemental analysis (SEM-EDX) of Inconel 625 substrate polarized in 1M KOH for 2 days at an applied potential of 1.8V, 2V, and 2.2V.....	22
Table 10: Elemental analysis (SEM-EDX) of Inconel 625 substrate polarized in alkaline artificial seawater for 2 days at an applied potential of 1.8V, 2V, and 2.2V at 50 °C.....	23
Table 11: Elemental analysis using SEM-EDX of C22 substrate polarized in 1M KOH at 1.6V at 50 °C for 7 days.....	24
Table 12: Elemental analysis (SEM-EDX) of C22 substrate polarized in alkaline ASW for 7 days at an applied potential of 1.6V, 1.8V, and 2V.....	26
Table 13: Elemental analysis using SEM-EDX of Ti substrate polarized in alkaline ASW for 7 days at an applied potential of -0.3V and -0.2V	27
Table 14: Elemental analysis using SEM-EDX of 316L substrate polarized in alkaline artificial seawater polarized for 7 days at an applied potential of -0.3V and -0.2V.....	28
Table 15: Elemental analysis (SEM-EDX) of Monel 400 substrate and polarized in alkaline ASW for 2 days at an applied potential of -0.3V compared to the pristine state.....	28
Table 16: Elemental analysis (SEM-EDX) of Inconel 600 substrate polarized in alkaline ASW for 2 days at an applied potential of -0.3V compared to the pristine state.....	29
Table 17: Elemental analysis (SEM-EDX) of Inconel 625 substrate polarized in alkaline ASW for 2 days at an applied potential of -0.3V	30
Table 18: Summary of both anodic and cathodic polarization reactions at 50 °C in 1M KOH and ASW	31



1 Introduction

Deliverable 5.1 “*Corrosion of uncoated BPP and PTL materials*” reports the results achieved within Work Task 5.1 (WT5.1) on the investigation of the ex situ corrosion testing of different uncoated substrates using three-electrode cells for a large matrix of experimental parameters: type of electrolyte (artificial and natural seawater), pH, potential (anodic and cathodic), temperature, etc. The activities presented in this deliverable cover the corrosion study of the bare metal substrates used to produce bipolar plates (BPP) and porous transport layers (PTL) of an AEM-based seawater electrolyser. This report summarises the corrosion investigation (up to one week) of the metals and alloy substrates in KOH as well as near-neutral and alkalized seawater conditions at 50-60°C using electrochemical and spectroscopic techniques.

2 Experimental

2.1 Methods

Substrate Materials

To determine the potential substrate material stable under corrosive seawater conditions, different metals and alloys were polarized anodically and cathodically. For the metallic substrate, pure nickel (Ni) and titanium (Ti) were used as received. For the potential metal alloys, some Ni-based and Fe-based alloys were used. The list of alloys with their compositions is tabulated in Table 1.

Table 1: Elemental composition of the different alloys (in wt%)

<i>Alloy</i>	<i>Ni</i>	<i>Cr</i>	<i>Mo</i>	<i>Fe</i>	<i>W</i>	<i>Mn</i>	<i>Cu</i>	<i>Co</i>	<i>Nb + Ta</i>	<i>Ti</i>
Inconel600	≥ 72	14 - 17		6 - 10		≤ 1	≤ 0.5	0 - 2	≤ 1	≤ 0.5
Inconel625	58	20 - 23	08 - 10	≤ 5		0.50		≤ 1	3.15 - 4.15	≤ 0.4
Monel400	≥ 63			≤ 2.5		≤ 2	28 - 34			
C-22	Bal.	20 - 22.5	12.5 - 14.5	2 - 6	2.5 - 3.5	≤ 0.5		≤ 2.5		
316L	10 - 14	16 - 18	02 - 03	Bal.		≤ 2				

Electrolytes

The electrolyte solutions used during the polarization reactions were KOH solutions with and without NaCl salt, and an alkaline artificial seawater (ASW) solution, prepared in the laboratory, mimicking the salt concentrations of natural seawater. The ASW is based on ASTM D1141-98(2021) standard, excluding any ions with concentrations lower than 0.1 g/L. As such, this doesn't include any form of heavy metal ions. The key ionic components are the Cl⁻ (seen as the main corrosive agent), Br⁻, as well as Mg²⁺ and Ca²⁺, which will form insoluble precipitates (in highly alkaline solutions), and CO₃²⁻, which may affect the conductivity of the membrane by disrupting the Grotthus mechanism of transport (likely more of an issue in AEM fuel cells). Na⁺ and K⁺ are present as the main cationic components of seawater.



For the preparation of 1M KOH in seawater (alkaline ASW), salts with weights according to Table 2 were dissolved in 0.8 L of deionized (DI) water. To this solution, 0.2 L of 5M KOH in water was slowly added under stirring. After 1 hour of stirring, the solution was filtered to ensure that no solid remained in the filtrate.

Table 2: Chemical composition of artificial seawater (mixed salts in 0.8L DI water)

Compound	Molecular Weight (g/mol)
NaCl	24.53
MgCl ₂ ·6H ₂ O	11.10
Na ₂ SO ₄ (anhydrous)	4.09
CaCl ₂ (anhydrous)	1.16
KCl	0.695
NaHCO ₃	0.201
KBr	0.101

Electrochemical characterization of substrates

The stability test of metal substrates was performed in a Teflon cell using a three-electrode setup. Preliminary experiments in glass cells revealed glass corrosion and sample contamination by a large amount of Si (not shown in this report). The substrates were placed at the bottom of the Teflon cell, and a polymer gasket was placed between the substrate and the cell to ensure no leakage of the electrolyte. The metal substrate served as the working electrode, the reversible hydrogen electrode (RHE) (or Hg/HgO (1M KOH)) as the reference electrode, and a mixed-metal oxide coated titanium mesh (or Pt mesh) as the counter electrode. All potentials reported in this deliverable are measured versus the RHE.

For the electrolyte solution, 1M KOH, 1M KOH with 0.6M Cl⁻ ion concentrations (0.6M NaCl), or alkaline artificial seawater (ASW) was used. The stability tests were conducted by applying a fixed potential of either 1.6V to 2.2V vs RHE at an operating temperature of 50 °C. Potentiostats (GAMRY Interface 1100E and BioLogic VSP-300) were utilized for the electrochemical analysis, and a thermal bath regulator (LAUDA) for maintaining the operating temperature. Initially, the open-circuit potential (OCP) is measured to stabilize the system. Then, chronoamperometry (CA) at a fixed potential was performed for a long duration.

Physicochemical characterization of substrates

The metal substrates were analysed both before and after the corrosion test to determine the stability in the electrolyte solution. The interfacial contact resistance (ICR) was measured with a copper contact pad at an applied clamping pressure of 1.5 MPa before and after the corrosion test (to be compared to the reference value of 10 mΩ·cm²), notably for evidencing a possible oxidation of the surface. Scanning electron microscopy (SEM) (HITACHI SU3500) was used to record top-view images for analysing the surface morphology of the substrate. For some samples, the corrosion products formed on the surface were identified using Raman spectroscopy (HORIBA XploRA PLUS) with a 533 nm laser. Energy dispersion X-ray spectroscopy (EDS) enabled the assessment of the chemical composition of the



substrate after the corrosion experiment, in particular to identify the growth of oxide layers. To determine the type of corrosion, if observed, and the extent of the surface damage, the polarized area was analyzed using a Profilometer (Wyko NT1100).

2.2 Anodic Polarization

All the metal substrates were anodically polarized in 1M KOH with and without chlorides at 50 °C. The applied potential was varied between 1.6V and 2.2V. The duration of the experiment was varied between a few hours and 7 days, based on the visible stability of the substrate in the electrolyte solution.

2.2.1 Nickel (Ni)

In 1M KOH (pH ~ 14)

Figure 1a shows the image of the Ni substrate after polarization in 1M KOH at 1.6V for 2 days. There is no visible damage to the surface of the Ni substrate, although the exposed surface was oxidized, leading to the discoloration of the surface. The SEM images of Ni (Figures 1b and 1c) reveal that the polarization does not cause any damage to the surface. More likely, there are some oxide (or hydroxide) products formed on the surface, as confirmed by EDX (Table 3). The ICR value of the polarized substrate was found to be similar to that of the pristine state, around $1 \text{ m}\Omega \cdot \text{cm}^2$.

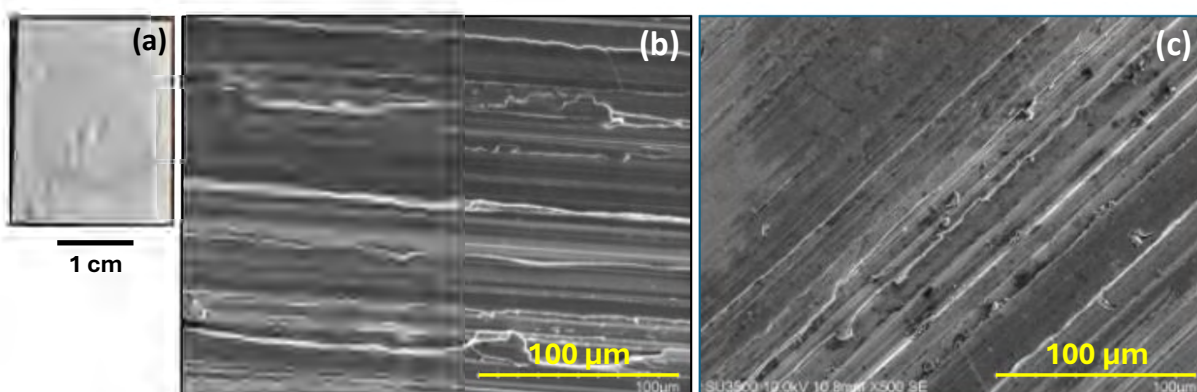


Figure 1: (a) Photograph of Ni substrate polarized for 2 days at 1.6V at 50 °C in 1M KOH. The exposed surface is the round-shaped area in the centre. The rest of the sample was not exposed to the electrolyte. SEM images of the Ni substrate in (b) the pristine state, and (c) after polarization.

Table 3: Elemental analysis (SEM-EDX) of Ni substrate polarized in 1M KOH at 1.6V at 50 °C for 2 days

Atom%	Ni	O
Pristine Ni	96.3	-
Polarized at 1.6V for 2 days	86.6	5.4

In Alkaline Artificial Seawater (pH ~ 14)

The alkaline ASW was prepared as described in Section 2.1 with pH ~14. The Ni substrates were polarized in ASW at 1.6V. The substrates were found to corrode within an hour of polarization, as the electrolyte solution was found to turn pale green after 45 minutes (Figure 2b). Figure 2a shows an image of the Ni substrate polarized for 45 mins in alkaline ASW, with no visible surface damage or corrosion

of the substrate. However, the SEM images (Figure 2c and 2d) reveal that polarization in ASW results in nickel dissolution due to the presence of the aggressive Cl^- ions. Those results show that, without being protected, Ni quickly degrades in the presence of chloride ions under anodic conditions.

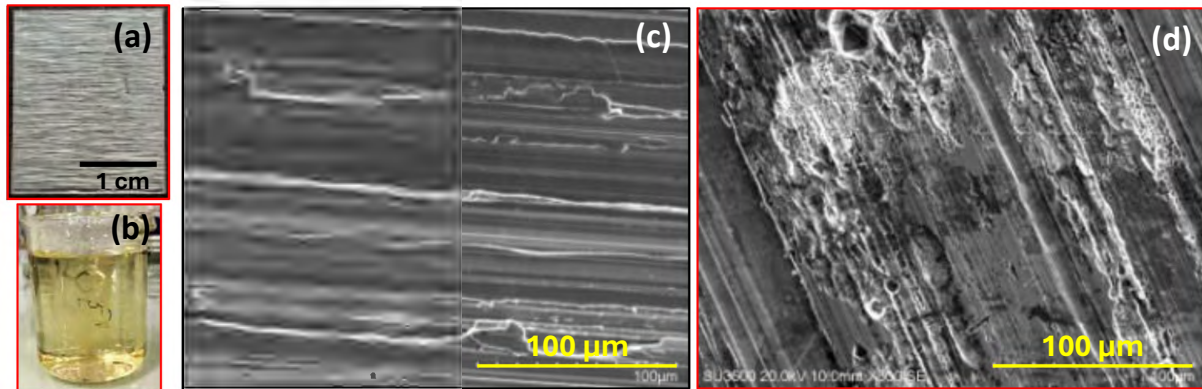


Figure 2: (a) Photograph of Ni substrate polarized in alkaline ASW for 45 mins at 1.6V at 50 °C. The exposed surface is the round-shaped area in the centre (barely visible in this picture). The rest of the sample was not exposed to the electrolyte. (b) The electrolyte solution after polarization. SEM images of the Ni substrate in (b) the pristine state, and (c) after polarization.

2.2.2 Titanium (Ti)

In 1M KOH (pH ~ 14)

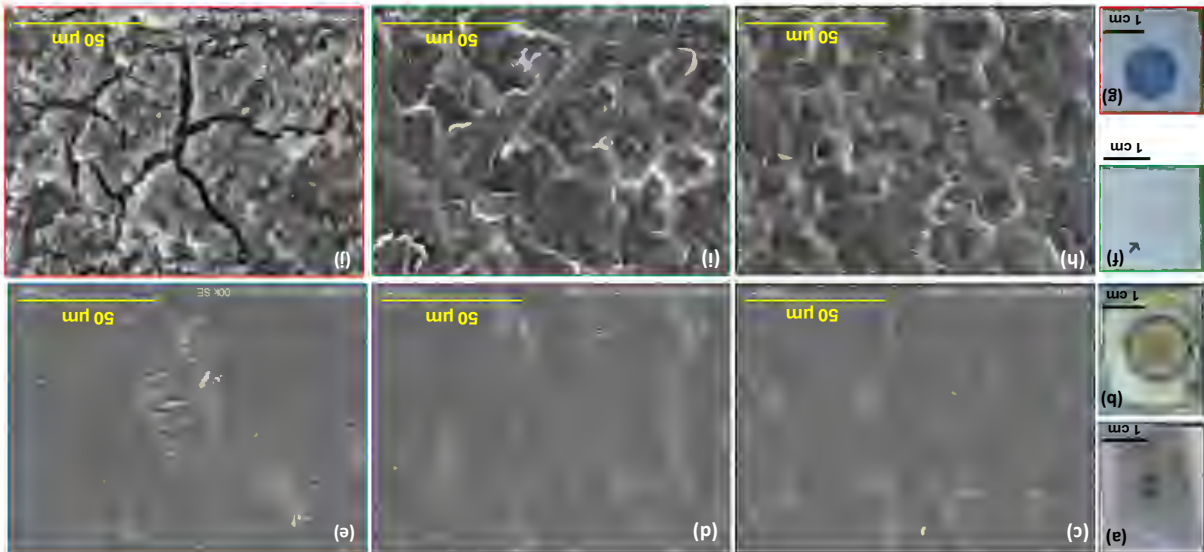
Figure 3a shows the image of the Ti substrate after polarization in 1M KOH at 1.6V for 2 days. Post-mortem naked-eye observation reveals no visible damage besides a discoloration associated with the oxidation (or hydroxylation) of the surface (as in the case of Ni). The SEM image of the Ti substrate shows no damage to the surface after polarization (Figure 3d, to be compared with Figure 3c of the pristine state). As the EDX could not detect any oxygen (Table 4), it is likely that the oxide/hydroxide layer responsible for the discoloration is very thin (< 100 nm). The ICR value was found to be similar to that of the pristine state (Table 6). For 7 days of polarization at 1.6V (Figure 3b), the oxide/hydroxide layer is sufficiently thick to be detected by EDX (Table 4), which probably relates to the slight increase in ICR value (Table 6). Yet, SEM micrographs do not show a significant change in the surface morphology (Figure 3e).

When the Ti substrate was subjected to harsher anodic conditions at 2.2V for 7 days (Figure 3g), the oxide/hydroxide layer became so thick that it exhibited cracks, as shown in Figure 3j (no damage was observed after 2 days, Figure 3f and 3i). For the 7-day polarization, EDX results (Table 4) reveal a Ti/O ratio close to that of TiO₂ or Ti(OH)₂, suggesting that the oxide/hydroxide layer is in the range of 1 μm thick. Such thickness allowed for a reliable Raman microscopy analysis revealing the characteristic peaks of the rutile phase, as shown in Figure 4.

Atom %		
Ti	O	
98.9	-	Pristine Ti
96.7	-	Polarized at 1.6V for 2 days
70.2	19.2	Polarized at 1.6V for 7 days
98.2	-	Polarized at 2.2V for 2 days
30.2	54.2	Polarized at 2.2V for 7 days

Table 4: Elemental analysis (SEM-EDX) of Ti substrate polarized in 1M KOH at 1.6V and 2.2V at 50 °C for 2 and 7 days

Figure 3: (a-e) Polarization of Ti substrate at 1.6V at 50 °C in 1M KOH. Photographs of the Ti substrate polarized for (a) 2 days and (b) 7 days. The exposed surface is the round-shaped area in the centre. SEM images in (c) pristine state, (d) after polarization for 2 days, and (e) after polarization for 7 days. (f-i) Polarization of Ti substrate at 2.2V at 50 °C in 1M KOH. Photographs of the Ti substrate polarized for (f) 2 days and (g) 7 days. The exposed surface is the round-shaped area in the centre. SEM images in (h) pristine state, (i) after polarization for 2 days, and (j) after polarization for 7 days.



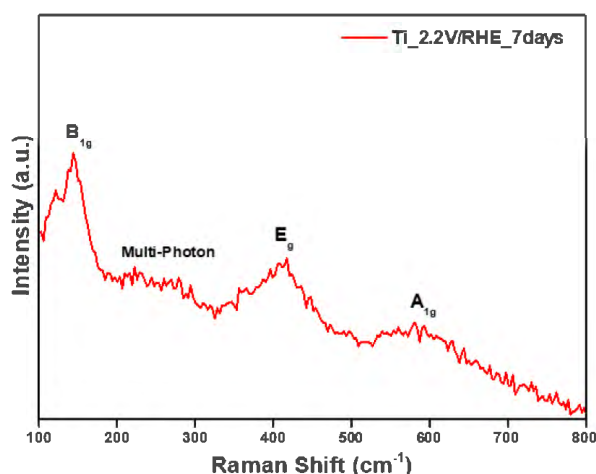


Figure 4: Raman spectra of Ti substrate polarized in 1M KOH at 2.2V at 50 °C for 7 days.

In Alkaline Artificial Seawater (pH ~14)

When tested in alkaline ASW, the titanium substrate behaved more or less the same way as in KOH (from a general and qualitative viewpoint). After 2 days of polarization at 1.6 V and 2.2 V, the surface did not exhibit significant damage (Figure 5a-e), oxygen is not detectable by EDX (Table 5), and ICR values (Table 6) remain low. After 7 days (Figures 5f and 5g), the oxide/hydroxide layers obtained at both potentials are thick, observable by SEM with the presence of cracks and spallation of layer fragments (Figures 5i and 5j). The presence of oxygen in the oxide/hydroxide layers is unambiguously evidenced by EDX (Table 5). The ICR is significantly higher (compared to their values after 2 days) (Table 6). This can be explained by the fragments of the oxide/hydroxide layer that peel off the substrates (or are loosely attached to them), which is detrimental for this type of measurement.

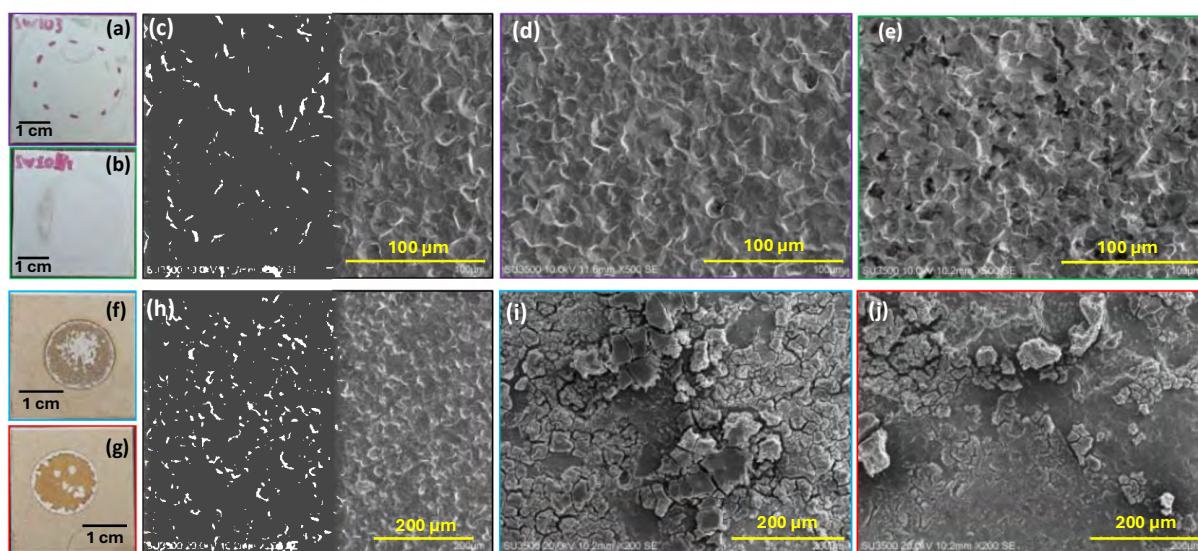


Figure 5: (a-e) Polarization for 2 days at 50 °C in alkaline ASW. Photographs of the Ti substrate polarized at (a) 1.6V and (b) 2.2V. The exposed surface is the round-shaped area in the centre. SEM images in (c) pristine state, (d) after polarization at 1.6V, and (e) after polarization at 2.2V.

(f-i) Polarization for 7 days at 50 °C in alkaline ASW. Photographs of the Ti substrate polarized at (f) 1.6V and (g) 2.2V. The exposed surface is the round-shaped area in the centre. SEM images in (h) pristine state, (i) after polarization at 1.6V, and (j) after polarization at 2.2V.

The thick layers obtained after 7 days were further analyzed using Raman spectroscopy (Figures 6a and 6b). In contrast to the results obtained in KOH, the Raman spectra show here the characteristic peaks of the anatase phase of TiO_2 (instead of rutile), confirming thereby the formation of an oxide layer on the surface of the Ti substrate when subjected to anodic polarization.

Table 5: Elemental analysis (SEM-EDX) of Ti substrate polarized in alkaline artificial seawater polarized for 2 days and 7 days at an applied potential of 1.6V and 2.2V

Atom%	Ti	O
<i>Pristine Ti</i>	99.2	-
<i>Polarized at 1.6V for 2 days</i>	96.9	-
<i>Polarized at 1.6V for 7 days</i>	27.7	61.1
<i>Polarized at 2.2V for 2 days</i>	98.8	-
<i>Polarized at 2.2V for 7 days</i>	41.9	45.7

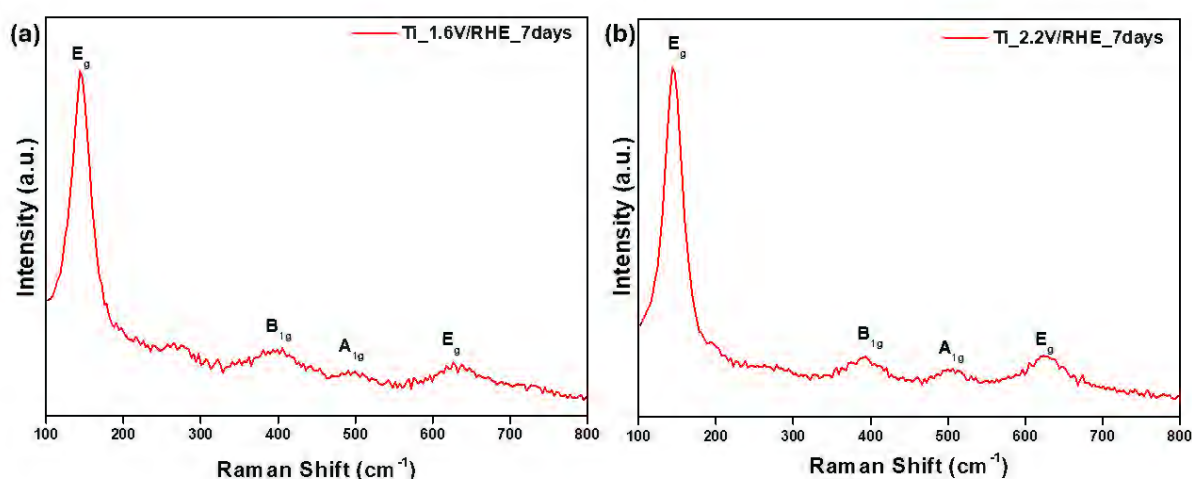


Figure 6: Raman spectra of Ti substrates polarized in alkaline artificial seawater at 50 °C for 7 days at an applied potential of (a) 1.6V and (b) 2.2V.

The Ti substrates polarized for 7 days at 2.2V in alkaline ASW (Figure 5g) were subsequently analyzed by profilometry to better understand the type of corrosion of the substrate. The line scan unambiguously reveals the formation of several pits (depth range: 20-40 μm) on the surface (Figure 7a). Thus, Ti undergoes pitting corrosion along with the formation of an oxide layer at highly anodic potential in alkaline ASW. For comparison, the profilometry line scan profile of the Ti substrate polarized at the same voltage and duration in 1M KOH suggests homogeneous metal dissolution and formation of a concave surface (max. depth $\sim 15 \mu\text{m}$, Figure 7b). The dissolution of the metal may be due to the release of TiO_4^{4-} or HTiO_4^{3-} anions. Further investigations are, however, needed to confirm or reject this assumption.

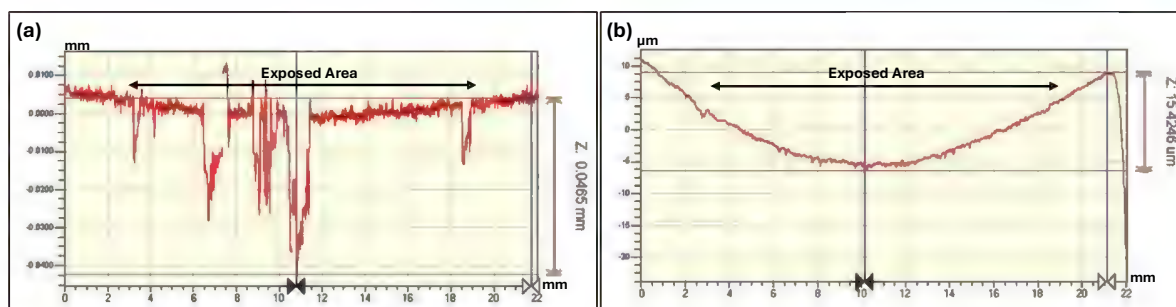


Figure 7: Profilometry line scan along the diameter of the exposed surface area for the Ti substrates polarized for 7 days at 2.2V in (a) alkaline ASW and (b) 1M KOH.

Table 6: Interfacial contact resistance (ICR) values of Ti substrates polarized at 1.6V and 2.2V for 2 and 7 days

Sample	Electrolyte	Potential	Duration	ICR ($\text{m}\Omega \cdot \text{cm}^2$)
Pristine Ti	-	-	-	1-2
Polarized Ti	1M KOH	1.6V	2 days	1-2
			7 days	4-5
		2.2V	2 days	1-2
			7 days	6-7
Polarized Ti	Alkaline ASW	1.6V	2 days	1-2
			7 days	58-62
		2.2V	2 days	1-2
			7 days	38-42

2.2.3 Stainless Steel (316L)

In 1M KOH (pH ~ 14)

The 316L was polarized in 1M KOH at 1.6V for 7 days at 50 °C. The polarized substrate is shown in Figure 8a. After 7 days of polarization, the electrolyte solution turned “yellow-brownish” (Figure 8d). The top-view SEM micrographs in pristine and polarized states are shown in Figures 8b and 8c, respectively. They show no significant damage, while EDX (Table 7) confirms the formation of oxides (and/or hydroxide) at the surface. Those findings suggest that during the oxidation/hydroxylation of the surface, leaching of 316L constituents (Fe, Cr, Ni) into the electrolyte solution occurs. Such leaching can be seen as a minor form of substrate corrosion, which still requires a coating on the 316L surface to be suppressed. Furthermore, the surface oxidation/hydroxylation leads to the ICR value increasing from $1 \text{ m}\Omega \cdot \text{cm}^2$ to $12 \text{ m}\Omega \cdot \text{cm}^2$.

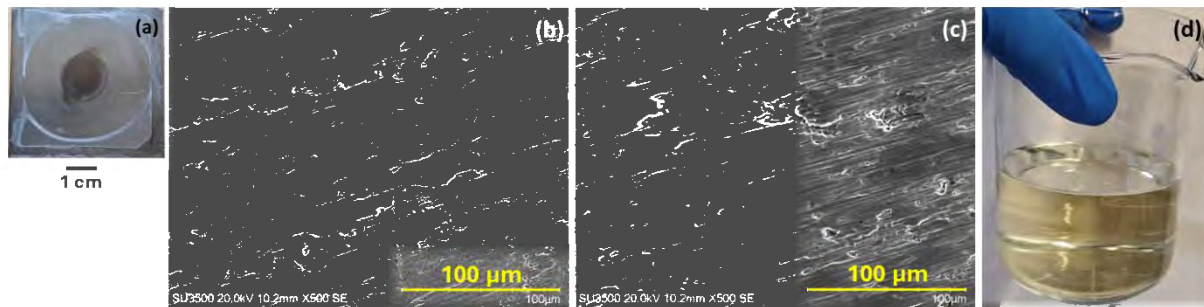


Figure 8: (a) Photograph of 316L substrate polarized for 7 days at 1.6V at 50 °C in 1M KOH. The exposed surface is the round-shaped area in the centre. The white marks along the side of the samples are remnants of the silicon gasket. SEM images of 316L substrate in (b) pristine state and (c) after polarization. (d) Photograph of the “yellow-brownish” electrolyte after polarization.

Table 7: Elemental analysis using SEM-EDX of 316L substrate polarized in 1M KOH at 1.6V at 50 °C for 7 days

Atom%	Fe	Cr	Ni	O	Mo
Pristine 316L	65.6	17.6	9.3	-	1.1
Polarized in 1M KOH	61.6	17.1	8.1	6.6	1.1

In Alkaline Artificial Seawater (pH ~ 14)

The bare 316L was also polarized at 1.6V at 50 °C in alkaline ASW. After 2 days of polarization, the colour of the electrolyte was observed to be reddish (Figure 9b), associated with the release of iron cations into the electrolyte and commonly observed for severe 316L corrosion. Pitting corrosion was evidenced by SEM imaging in the middle of the exposed area (Figure 9d and 9e, to be compared to the pristine state of Figure 9c). At the same time, one large crevice was observed under the gasket of the cell, leading to a small leakage of the electrolyte outside the cell, visible in Figure 9a. 316L is known to corrode in the presence of chloride in acidic and near-neutral solutions. The present findings show that this is also the case at pH around 14.

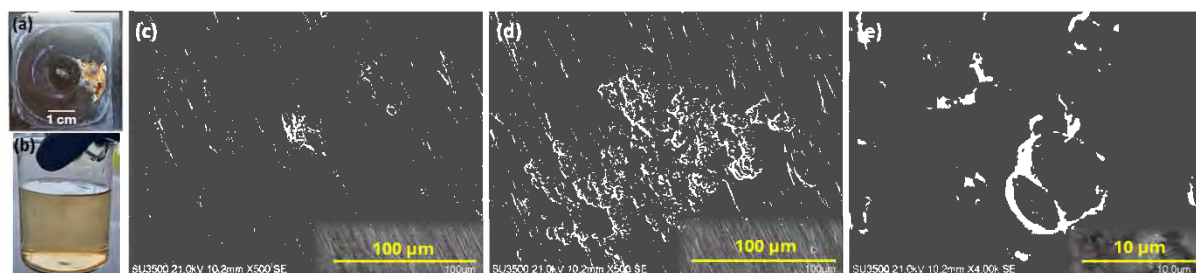


Figure 9: (a) Photograph of 316L substrate polarized for 2 days in alkaline artificial seawater at 1.6V at 50 °C. The exposed surface is the round-shaped area in the centre. (b) Photograph of the reddish electrolyte after polarization. SEM images of 316L substrate in (c) pristine condition and (d & e) after polarization.



2.2.4 Monel 400

In 1M KOH + 0.6 M NaCl solution (pH ~ 14)

Monel 400 was the first nickel-based alloy investigated in this study. Unlike the other nickel-based alloys reported in Table 1, it does not contain any chromium, which is a key-element for forming a (protective) passive layer. In 1M KOH + 0.6 M NaCl solution (mimicking the chloride concentration of seawater) at 50 °C for 2 days, the alloy was stable at a polarization of 1.7V with no sign of significant degradation (Figure 10a), but was heavily corroded at 1.9V with the presence of large pits (Figure 10b). It was decided not to pursue investigations with alloy and focus attention on chromium-containing nickel-based alloys (see below).

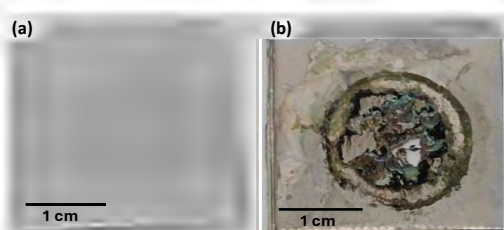


Figure 10: Photographs of Monel 400 substrates polarized at 50 °C for 2 days at an applied potential of (a) 1.7V and (b) 1.9V. The exposed surface is the round-shaped area in the centre.

2.2.5 Inconel 600

In 1M KOH (pH ~ 14)

Inconel 600 was tested in 1 M KOH at 50 °C for 2 days at potentials of 1.8V, 2V, and 2.2V. Figures 11a, 11d, and 11g show the polarized substrates with the corresponding SEM images (Figures 11c, 11f, and 11i). When compared to the SEM images of their pristine states (Figures 11b, 11e, and 11h), no signs of degradation were observed at all the potentials. The EDX analysis (Table 8) reveals the absence of oxygen for all substrates, indicating that the substrates did not undergo significant oxidation/hydroxylation during anodic polarization. The decrease of Ni, Cr, and Fe content of the polarized substrates (compared to the pristine state values) is an artefact explained by carbon contamination (ca. 17-20 atom%) before or during EDX analysis. These findings confirm the stability of the Inconel 600 under anodic polarization in 1M KOH at 50 °C.

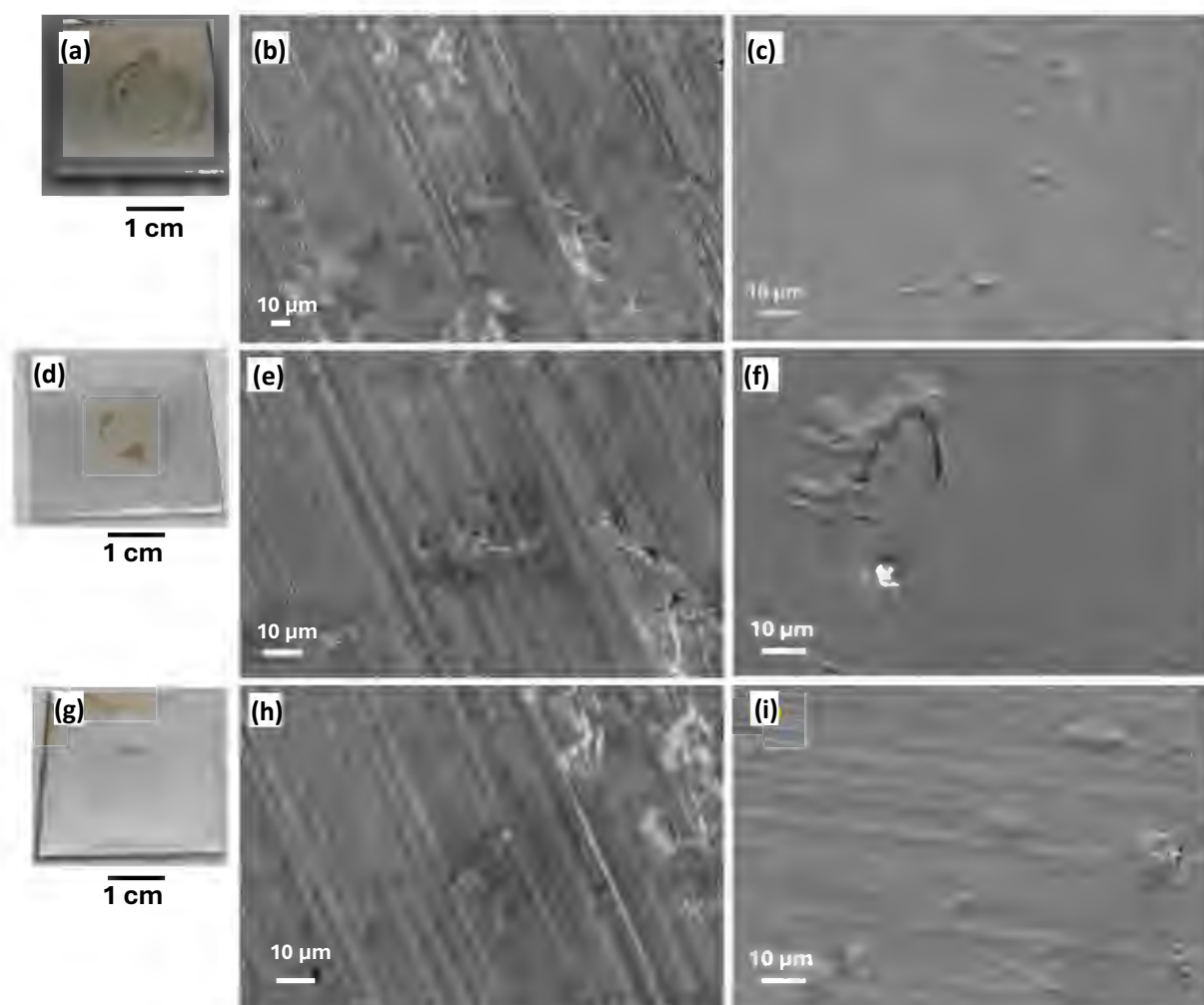


Figure 11: (a-c) **Polarization at 1.8V at 50 °C in 1M KOH.** (a) Photograph of Inconel 600 substrate polarized for 2 days. The exposed surface is the round-shaped area in the centre. SEM images of (b) pristine state, and (c) after polarization. (d-f) **Polarization at 2V at 50 °C in 1M KOH.** (d) Photograph of Inconel 600 substrate polarized for 2 days. The exposed surface is the round-shaped area in the centre. SEM images of (e) pristine state, and (f) after polarization. (g-i) **Polarization at 2.2V at 50 °C in 1M KOH.** (g) Photograph of Inconel 600 substrate polarized for 2 days. The exposed surface is the round-shaped area in the centre. SEM images of (h) pristine state, and (i) after polarization.

Table 8: Elemental analysis (SEM-EDX) of Inconel 600 substrate polarized in 1M KOH for 2 days at an applied potential of 1.8V, 2V, and 2.2V

Atom%	Ni	Cr	O	Fe	C
Pristine Inconel 600	70.90	15.70	-	8.0	5.40
Polarized at 1.8V	59.68	14.26	-	7.92	17.60
Polarized at 2V	58.41	13.74	-	7.61	19.72
Polarized at 2.2V	57.95	13.45	-	7.55	20.34

In Alkaline Artificial Seawater (pH ~ 14)

The Inconel 600 substrates were tested in alkaline ASW for 2 days under the same experimental conditions (potentials of 1.8V, 2V, and 2.2V) as in the IM KOH solution. The substrates exhibited strong corrosion damage (Figure 12). This indicates that Inconel 600 is not stable under anodic polarization in seawater (i.e., in the presence of chloride ions). SEM or EDX analyses were not performed on these samples as the degradation was visible on the surface.

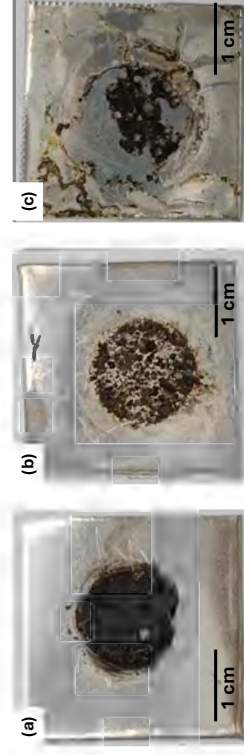


Figure 12: Photographs of Inconel 600 substrates polarized at 50 °C in alkaline artificial seawater for 2 days at (a) 1.8V, (b) 2V, and (c) 2.2V. The exposed surface is the round-shaped area in the centre.

2.2.6 Inconel 625

In 1M KOH (pH ~ 14)

The Inconel 625 was polarized in 1M KOH at 1.8V, 2V, and 2.2V for 2 days. Figures 13a, 13d, and 13f show the polarized substrates, with the corresponding SEM images. The SEM images for Inconel 625 polarized at 1.8V (Figure 13c) and 2V (Figure 13e) do not show any traces of possible oxide/hydroxide particles or any damage to the surface when compared to the pristine state (Figure 13b), but the EDX analysis (Table 9) shows the presence of oxygen atoms on its surface. The SEM image for the polarized substrate at 2.2V (Figure 13g) shows the thick oxide (hydroxide) layer, which is also validated by the EDX analysis. At lower potentials of 1.8V and 2V, a very thin oxide or hydroxide layer may have formed (based on the EDX results) on the surface, which was not beyond the resolution of the SEM analysis. But at the anodic potential of 2.2V, the formed oxide (or hydroxide) layer on the surface of Inconel 625 is thick enough to be resolved by the SEM analysis. Thus, Inconel 625 undergoes surface oxidation under anodic polarization in 1M KOH.

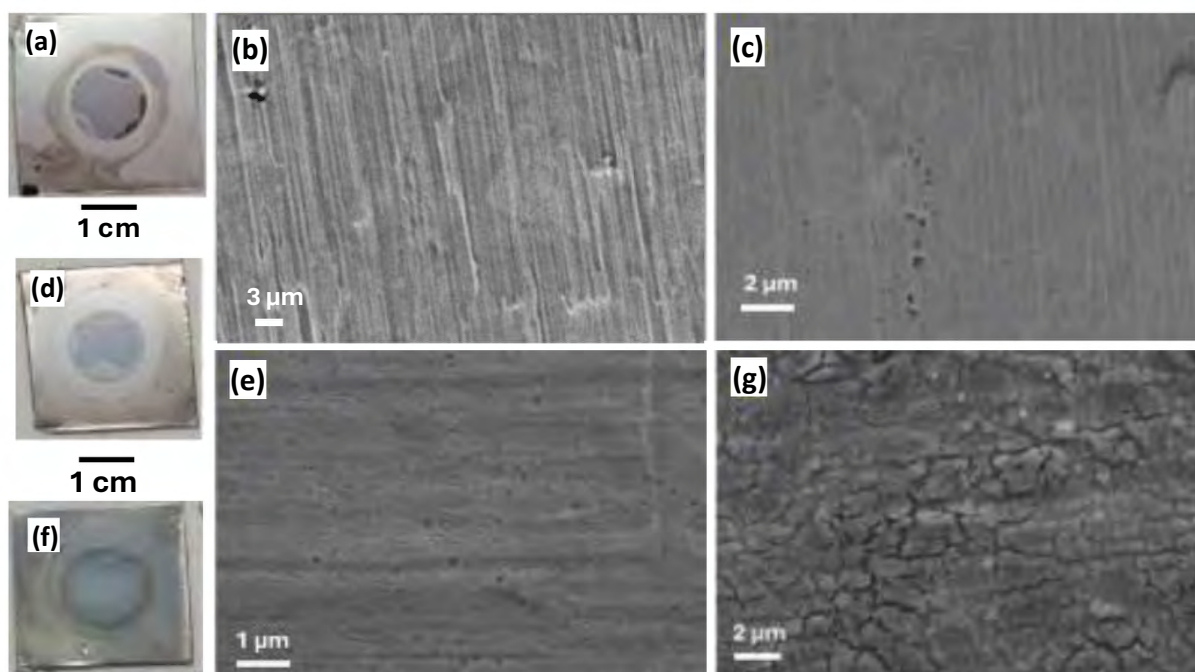


Figure 13: (a-c) **Polarization at 1.8V at 50 °C in 1M KOH.** (a) Photograph of Inconel 625 substrate polarized for 2 days. The exposed surface is the round-shaped area in the centre. SEM images of (b) pristine Inconel 625 and (c) after polarization. (d-e) **Polarization at 2V at 50 °C in 1M KOH.** (d) Photograph of Inconel 625 substrate polarized for 2 days. The exposed surface is the round-shaped area in the centre. (e) SEM image after polarization. (f-g) **Polarization at 2.2V at 50 °C in 1M KOH.** (f) Photograph of Inconel 625 substrate polarized for 2 days. The exposed surface is the round-shaped area in the centre. (g) SEM image after polarization.

Table 9: Elemental analysis (SEM-EDX) of Inconel 625 substrate polarized in 1M KOH for 2 days at an applied potential of 1.8V, 2V, and 2.2V

Atom%	Ni	Cr	Mo	O	Fe	Nb
Pristine Inconel 625	61.43	25.05	5.49	-	4.13	2.23
Polarized at 1.8V	54.14	21.72	4.69	13.07	3.57	1.82
Polarized at 2V	53.16	21.3	4.61	14.27	3.49	1.71
Polarized at 2.2V	38.14	13.92	2.85	39.89	2.35	1.31

In Alkaline Artificial Seawater (pH ~ 14)

The Inconel 625 substrates were exposed to alkaline ASW at 50 °C and polarized at 1.8V, 2V, and 2.2V for 2 days. All three substrates showed the formation of dark deposited layers on the surface after the polarization tests, as observed in Figures 14a, 14d, and 14f. The corresponding SEM images (Figures 14c, 14e, and 14g) show the presence of the thick oxide (or hydroxide) layers on the polarized surfaces when compared to their pristine state (Figure 14b). To confirm the surface oxidation, EDX analysis was performed, and the results are summarized in Table 10. The results also show the presence of a significant amount of Ca on the surface (5-15 atom%) that might have been incorporated during the building of the oxide/hydroxide layer. Further investigations are needed to clarify this point.

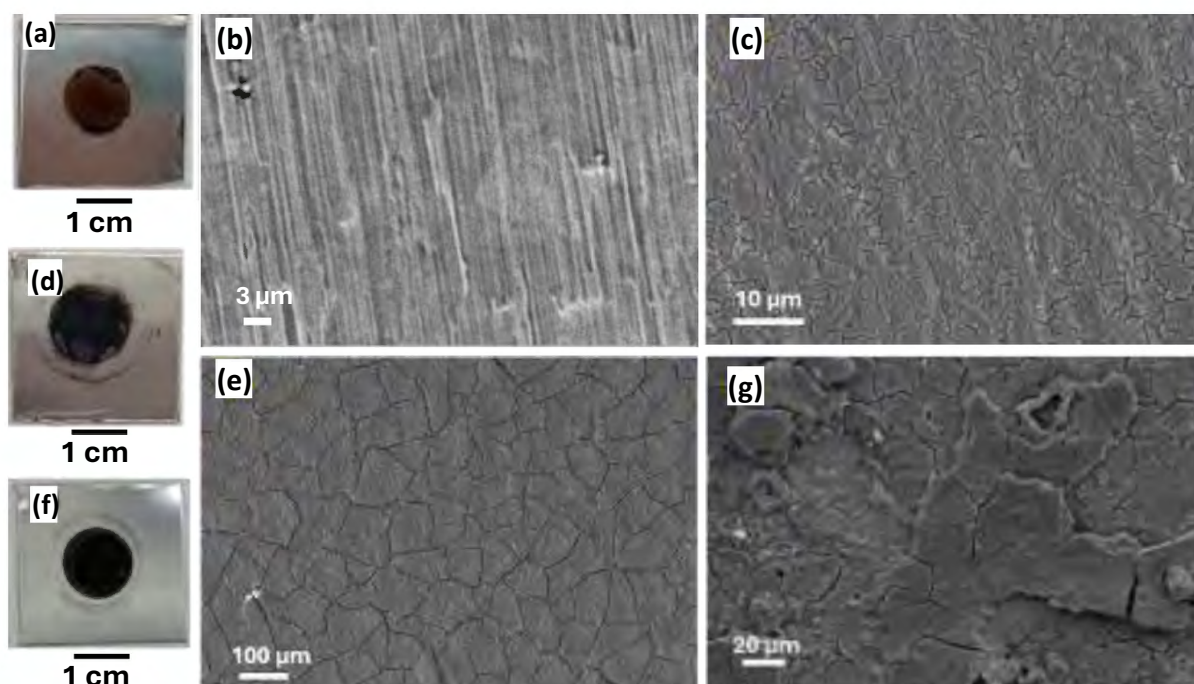


Figure 14: (a-c) **Polarization at 1.8V at 50 °C in alkaline ASW.** (a) Photograph of Inconel 625 substrate polarized for 2 days. The exposed surface is the round-shaped area in the centre. SEM images of (b) pristine Inconel 625 and (c) after polarization. (d-e) **Polarization at 2V at 50 °C in alkaline ASW.** (d) Photograph of Inconel 625 substrate polarized for 2 days. The exposed surface is the round-shaped area in the centre. (e) SEM image after polarization. (f-g) **Polarization at 2.2V at 50 °C in alkaline ASW.** (f) Photograph of Inconel 625 substrate polarized for 2 days. The exposed surface is the round-shaped area in the centre. (g) SEM images after polarization.

Table 10: Elemental analysis (SEM-EDX) of Inconel 625 substrate polarized in alkaline artificial seawater for 2 days at an applied potential of 1.8V, 2V, and 2.2V at 50 °C

Atom%	Ni	Cr	Mo	O	Fe	Ca
Pristine Inconel 625	61.21	25.04	5.49	-	4.13	-
Polarized at 1.8V	30.69	10.98	2.22	46.85	1.86	4.51
Polarized at 2V	13.95	0.77	0.16	66.71	0.58	16.51
Polarized at 2.2V	13.6	1.25	0.26	68.42	0.6	14.89

This suggests that Inconel 625, unlike Inconel 600, does not corrode heavily in the presence of chloride ions, but there is the formation of a thick oxide (or hydroxide) layer on the surface when polarized anodically.

2.2.7 C22 Alloy

In 1M KOH (pH ~ 14)

The C22 alloy was polarized in 1M KOH at 1.6V for 7 days. The C22 substrates had to be polished (down to P1200 paper) to remove an adhesive film present in the as-received state. Figure 15a shows the image of the polarized C22 substrate exhibiting a surface discoloration. The SEM images of the



surface in pristine and post-mortem states are shown in Figure 15b and 15c. They evidence the absence of significant corrosion damages while the EDX analysis (Table 11) reveals the presence of oxygen atoms on the surface, which is associated with oxidation/hydroxylation. The latter is believed to be the cause of the significant increase in the ICR from $1 \text{ m}\Omega\cdot\text{cm}^2$ (pristine state) to $14 \text{ m}\Omega\cdot\text{cm}^2$ (after polarization).

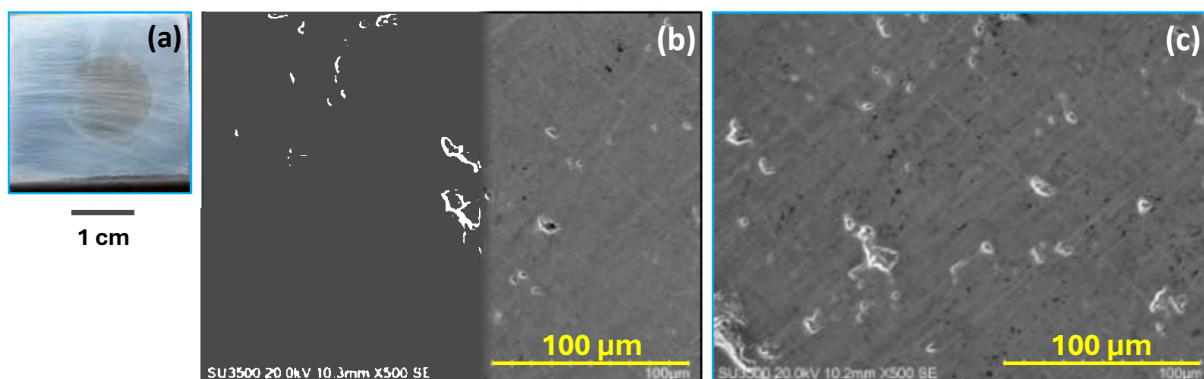


Figure 15: (a) Photograph of C22 substrate polarized in 1M KOH for 7 days at 1.6V at 50 °C. The exposed surface is the round-shaped area in the centre. SEM images in (b) the pristine state, and (c) after polarization.

Table 11: Elemental analysis using SEM-EDX of C22 substrate polarized in 1M KOH at 1.6V at 50 °C for 7 days

Atom%	Ni	Cr	Fe	O	Co	Mo	W
Pristine C22	56.6	21.8	3.9	-	1.2	7.7	1.3
Polarized C22	53.5	13.0	3.7	8.9	1.1	8.0	1.1

In Alkaline Artificial Seawater (pH ~ 14)

The C22 alloy was polarized in alkaline ASW at a potential of 1.6V, 1.8V, and 2V at 50 °C for 7 days. As can be seen from Figure 16a, the surface of the C22 is not affected in alkaline ASW under anodic polarization at 1.6V. The ICR value was found to be low ($\sim 3 \text{ m}\Omega\cdot\text{cm}^2$) and comparable to the pristine state ($\sim 1 \text{ m}\Omega\cdot\text{cm}^2$). The SEM images (Figures 16b & 16c) also confirm the stability of the C22 alloy under polarization in alkaline ASW at 1.6V, as there was no visible damage to the surface. At a higher polarization potential of 1.8V and 2V in alkaline ASW for 7 days, the C22 substrates seem to have corroded (Figures 16d and 16f). There was a thick oxide (or hydroxide) layer formation on the surface, as can be seen in the SEM images (Figures 16e and 16g). Thus, C22 is only stable at a lower potential of 1.6V for 7 days in alkaline ASW. The visible damage around the exposed area at the centre of the C22 substrates polarized at 1.8V and 2V (Figures 16d & 16f) is due to the crevice corrosion under the confined region of the gasket, which led to the pale green colouration of the electrolyte solution.

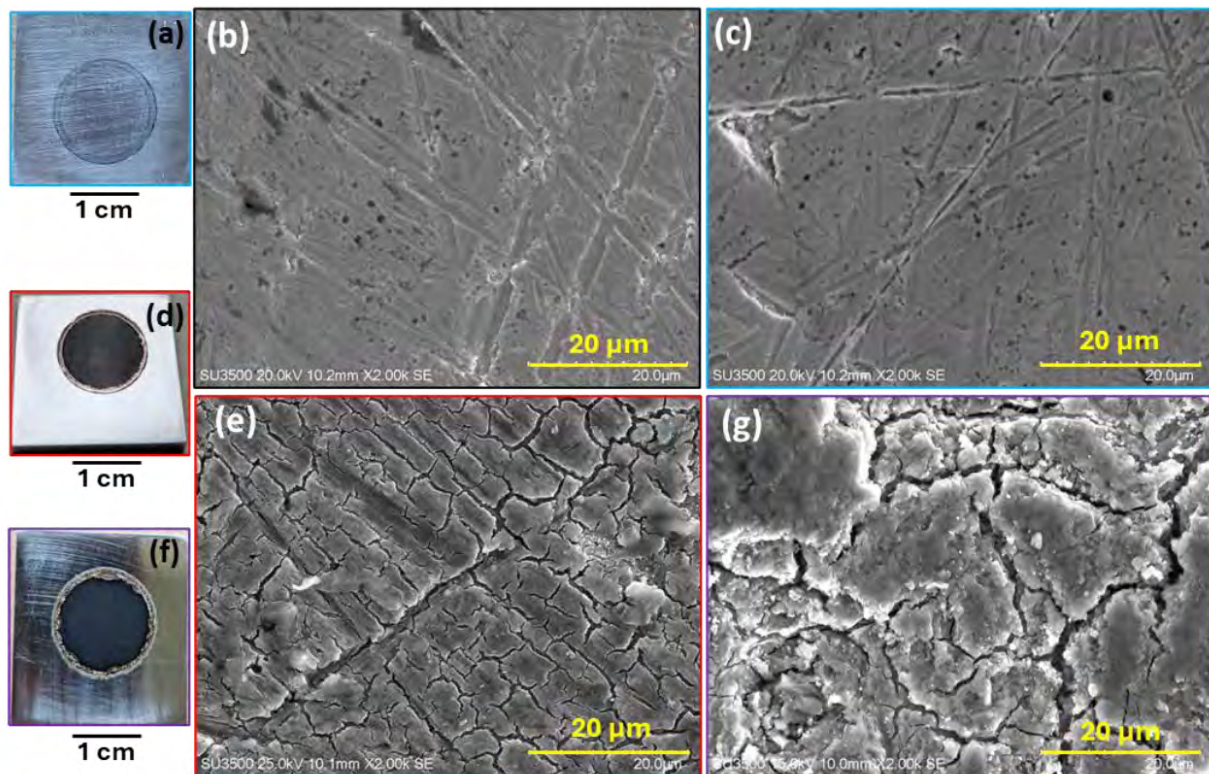


Figure 16: (a-c) **Polarization at 1.6V at 50 °C in alkaline ASW.** (a) Photograph of C22 substrate polarized for 7 days. The exposed surface is the round-shaped area in the centre. SEM images of C22 in (b) pristine state, (c) after polarization. (d, e) **Polarization at 1.8V at 50 °C in alkaline ASW.** (d) Photograph of C22 substrate polarized for 7 days. The exposed surface is the round-shaped area in the centre. (e) SEM image of C22 after polarization. (f, g) **Polarization at 2V at 50 °C in alkaline ASW.** (f) Photograph of C22 substrate polarized for 7 days. The exposed surface is the round-shaped area in the centre. (g) SEM image of C22 after polarization.

EDX analysis was performed on the polarized C22 substrate to detect the extent of oxidation of the surface after 7 days of anodic polarization. Table 12 shows the elemental composition of the C22 substrate in the pristine state and after polarization in ASW for 7 days at 1.6V, 1.8V, and 2V. EDX results show the presence of oxygen atoms on the C22 surface due to the anodic polarization in ASW. At 1.6V, the oxide (or hydroxide) layer may be too thin to be seen under SEM and has minimal influence on the ICR value. But at 1.8V and 2V, the oxide (or hydroxide) layer is thick enough to be seen under SEM and drastically increases the ICR. The ICR was found to increase drastically to $>100 \text{ m}\Omega \cdot \text{cm}^2$ due to the oxide (or hydroxide) layer formation on the surface of both C22 substrates.

The C22 substrates polarized for 7 days at 1.8V and 2V in alkaline ASW (Figures 16d and 16f) were analyzed using a Profilometer to determine the type of corrosion of the substrate. The profilometry line profile (Figure 17a) of the C22 substrate polarized at 1.8V confirms the absence of any pits and formation of an oxide (or hydroxide) layer. The profilometry line profile (Figure 17b) of the C22 substrate polarized at 2V confirms the outward growth of the oxide (or hydroxide) layer. The average thickness of the oxide (or hydroxide) layer is $\sim 9 \mu\text{m}$. The depths at the extremities of the line scan correspond to the crevice corrosion under the gasket. This aspect is not developed in this deliverable, but will be the one topic of in-depth investigations in WT5.4.

Table 12: Elemental analysis (SEM-EDX) of C22 substrate polarized in alkaline ASW for 7 days at an applied potential of 1.6V, 1.8V, and 2V

Atom%	Ni	Cr	Fe	O	Co	Mo	W
<i>Pristine C22</i>	57.0	19.0	4.2	-	1.2	7.8	3.0
<i>Polarized at 1.6V</i>	51.7	16.2	3.4	11.2	1.1	7.5	1.4
<i>Polarized at 1.8V</i>	24.1	11.2	1.5	48.4	0.6	2.6	1.5
<i>Polarized at 2V</i>	20.0	7.9	0.9	60.5	0.4	0.2	0.3

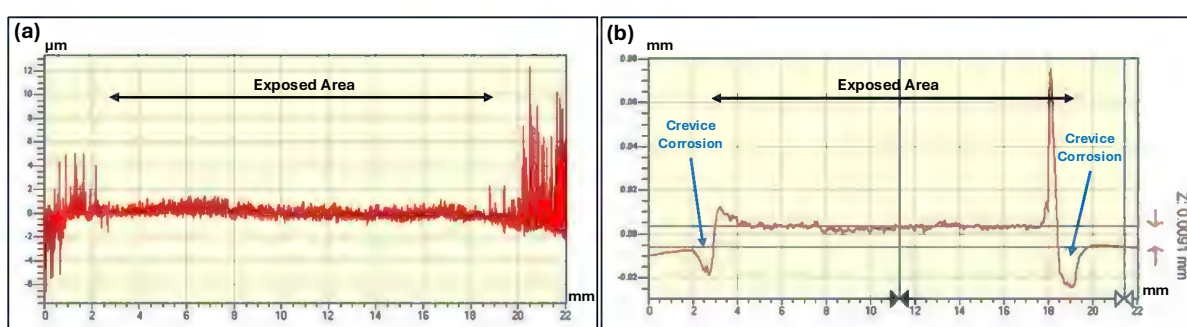


Figure 17: Profilometry line scan along the diameter of the exposed surface area for the C22 substrates polarized for 7 days in alkaline ASW at (a) 1.8V and (b) 2V. The large noise at both ends of the line scan (a) is due to gasket pieces sticking to the substrate after cell dismantling.

2.3 Cathodic Polarizations

The cathodic stability test of the metallic and alloy substrates and metal alloys was performed similarly to the anodic polarization tests in alkaline ASW at 50 °C. The applied potential was either $-0.3V$ or $-0.2V$ for 2 to 7 days.

2.3.1 Titanium (Ti)

In Alkaline Artificial Seawater (pH ~ 14)

The Ti substrate was polarized at both $-0.3V$ and $-0.2V$ for 7 days at 50 °C. In both cases, a discoloration of the substrate was clearly visible with naked-eye observation (Figures 18a and 18b). The SEM analysis shows no significant damage to the substrates, such as pitting or dissolution (Figure 18d and 18e, to be compared with the pristine state (Figure 18c)). The EDX analysis (Table 13) of both samples indicates a large amount of oxygen on the surface, which is in line with the oxide/hydroxide layer formation seen in Figures 18a and 18b. This layer formation is associated with a drastic increase in ICR from $1 \text{ m}\Omega \cdot \text{cm}^2$ for the pristine sample to 22-24 $\text{m}\Omega \cdot \text{cm}^2$ for the polarized ones. This suggests that an appropriate protective coating would be needed to keep ICR at low levels.

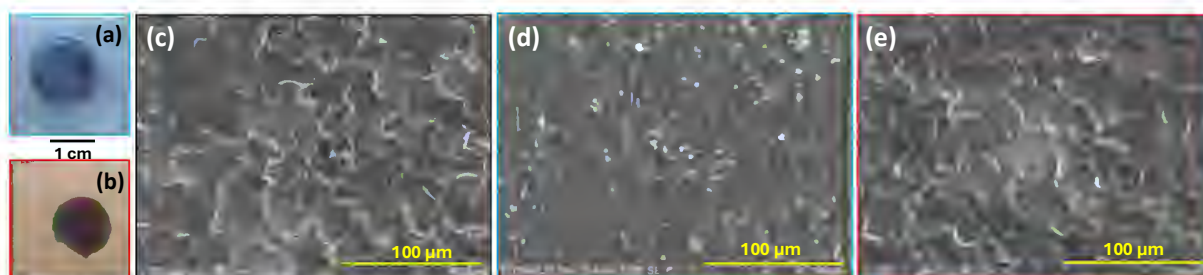


Figure 18: Photographs of Ti substrates polarized in alkaline ASW at 50 °C for 7 days at a potential of (a) $-0.3V$ and (b) $-0.2V$. The exposed surface is the round-shaped area in the centre. SEM images of Ti substrates in (c) pristine state, and after 7 days of polarization at (d) $-0.3V$ and (e) $-0.2V$.

Table 13: Elemental analysis using SEM-EDX of Ti substrate polarized in alkaline ASW for 7 days at an applied potential of $-0.3V$ and $-0.2V$

Atom%	Ti	O	Mg	Ca
<i>Pristine Ti</i>	98.6	-	-	-
<i>Polarized at $-0.3V$</i>	47.7	36.1	0.1	0.4
<i>Polarized at $-0.2V$</i>	44.3	43.9	0.4	0.2

2.3.2 Stainless Steel (316L)

In Alkaline Artificial Seawater (pH ~ 14)

The stainless steel (316L) was polarized in alkaline ASW at an applied potential of $-0.3V$ and $-0.2V$ for 7 days at 50 °C. From Figures 19a & 19b, it was observed that the 316L substrate was not affected in alkaline ASW under cathodic conditions at both potentials. The SEM images (Figure 19c-e) also confirm the stability of the substrate under the cathodic polarization for 7 days with no deposits of cathodic products. The ICR values of the polarized substrates (Figures 19a & 19b) were found to be $4 \text{ m}\Omega \cdot \text{cm}^2$ and $3 \text{ m}\Omega \cdot \text{cm}^2$, respectively.

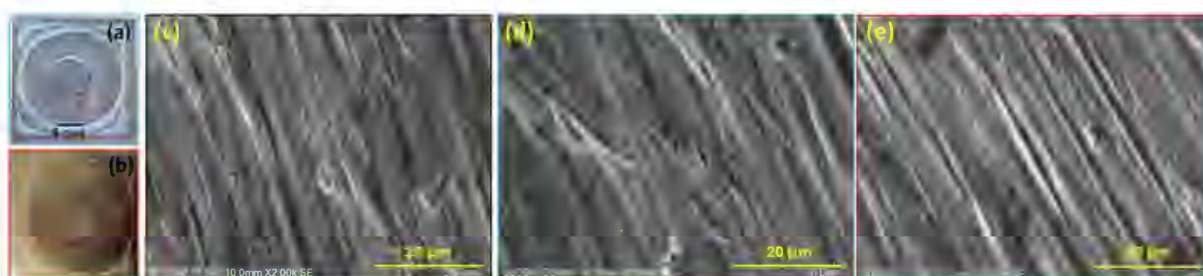


Figure 19: Photographs of 316L substrates polarized in alkaline ASW at 50 °C for 7 days at (a) $-0.3V$ and (b) $-0.2V$. The exposed surface is the round-shaped area in the centre. SEM images of 316L substrates in (c) the pristine state and after 7 days of polarization at (d) $-0.3V$ and (e) $-0.2V$.

The EDX analysis of the polarized 316L substrates is tabulated in Table 14. It shows that the elemental compositions of the substrates were found to be similar to those of the pristine 316L substrate. This further confirms the stability of the 316L substrate in alkaline ASW under cathodic conditions.



Table 14: Elemental analysis using SEM-EDX of 316L substrate polarized in alkaline artificial seawater polarized for 7 days at an applied potential of $-0.3V$ and $-0.2V$

Atom%	Fe	Cr	O	Mn	Ni
<i>Pristine 316L</i>	59.3	15.9	2.9	1.1	7.8
<i>Polarized at $-0.3V$</i>	56.4	15.1	9.7	0.9	7.5
<i>Polarized at $-0.2V$</i>	57.0	15.2	9.6	1.0	7.5

2.3.3 Monel 400

In Alkaline Artificial Seawater (pH ~ 14)

Monel 400 was cathodically polarized at $-0.3V$ for 2 days at $50\text{ }^{\circ}\text{C}$. As shown in Figure 20a, the substrates show no degradation or deposition of any cathodic products. The SEM image (Figure 20c) shows a clean surface with no deposits, when compared to its pristine state (Figure 20b). This confirms the stability of the Monel 400 under such experimental conditions. The stability of the polarized substrate has been confirmed using EDX. Table 15 shows the minimal presence of oxygen atoms after the polarization reaction.

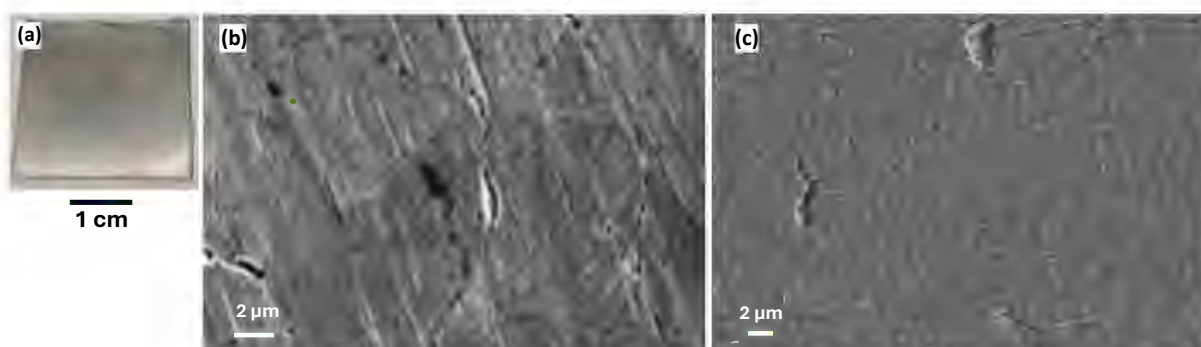


Figure 20: (a) Photograph of Monel 400 substrate polarized in alkaline ASW for 2 days at an applied potential of $-0.3V$. The exposed surface is the round-shaped area in the centre. The SEM images of (b) the pristine Monel 400, and (c) after polarization.

Table 15: Elemental analysis (SEM-EDX) of Monel 400 substrate and polarized in alkaline ASW for 2 days at an applied potential of $-0.3V$ compared to the pristine state

Atom %	Ni	Cu	O	Fe
<i>Pristine Monel 400</i>	64.7	31.2	1.4	2.0
<i>Polarized at $-0.3V$</i>	62.9	31.9	2.8	1.5

2.3.4 Inconel 600

In Alkaline Artificial Seawater (pH ~ 14)

Inconel 600 substrate was polarized in alkaline ASW at a potential of $-0.3V$ for 2 days at $50\text{ }^{\circ}C$. From Figure 21a, the exposed area exhibits a whitish discoloration, indicating the growth of oxide (or hydroxide) on the surface. The SEM image of the polarized substrate (Figure 21c), compared to the pristine state (Figure 21b), reveals the presence of multiple islands of deposits that may be the nucleation sites of oxides/hydroxides. EDX analysis did not reveal any incorporation of seawater elements (Mg, Ca, Na, Cl, etc.) in those deposits (Table 16).

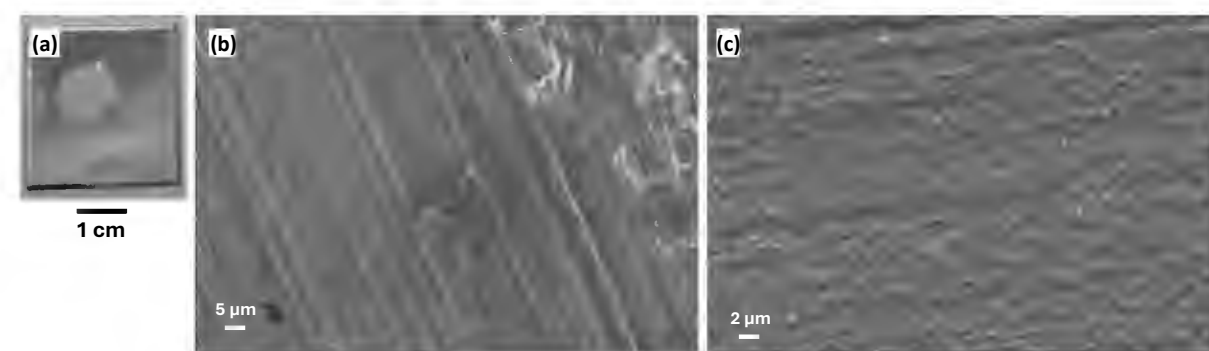


Figure 21: (a) Photograph of Inconel 600 substrate polarized in alkaline ASW for 2 days at an applied potential of $-0.3V$. The exposed surface is the round-shaped area in the centre. SEM images of (b) the pristine Inconel 600 and (c) after polarization.

Similarly, as earlier, the presence of oxygen on the surface has been confirmed using EDX analysis. Table 16 shows the presence of oxygen on the surface of the Inconel 600 after the cathodic polarization.

Table 16: Elemental analysis (SEM-EDX) of Inconel 600 substrate polarized in alkaline ASW for 2 days at an applied potential of $-0.3V$ compared to the pristine state

Atom %	Ni	Cr	O	Fe
Pristine Inconel 600	68.00	16.60	-	9.0
Polarized at $-0.3V$	50.29	12.20	8.75	6.73

2.3.5 Inconel 625

In Alkaline Artificial Seawater (pH ~ 14)

The stability of Inconel 625 alloys was evaluated at $-0.3V$ at $50\text{ }^{\circ}C$ for 2 days. Post-mortem naked-eye observation revealed no significant damage and no discoloration of the surface (Figure 22a). Yet, the EDX analysis (Table 17) shows the presence of a large amount of oxygen. The SEM image of the polarized substrate (Figure 22c), compared to the pristine state (Figure 22b), suggests that oxygen is concentrated in the homogeneously distributed light-contrast dots that may be nucleation sites of the oxide/hydroxide layer.

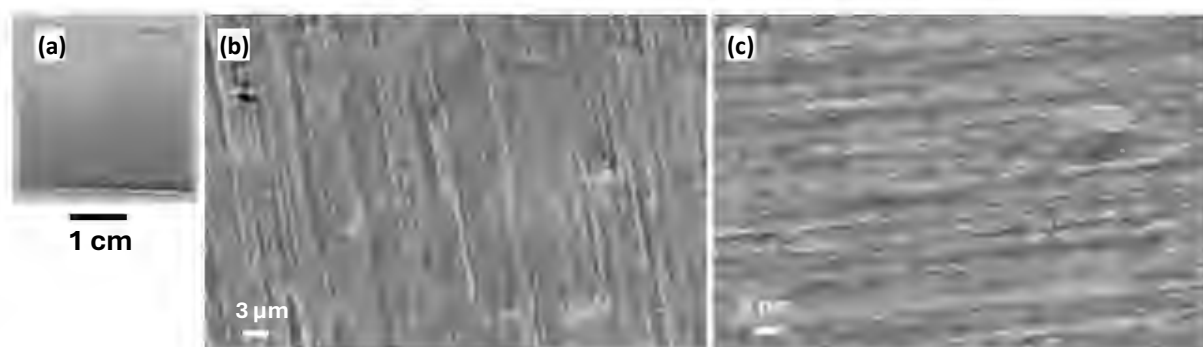


Figure 22: (a) Photograph of polarized Inconel 625 substrate in alkaline ASW for 2 days at an applied potential of $-0.3V$. The exposed surface is the round-shaped area in the centre. The SEM images of the (b) pristine state, and (c) after polarization.

Table 17: Elemental analysis (SEM-EDX) of Inconel 625 substrate polarized in alkaline ASW for 2 days at an applied potential of $-0.3V$

Atom %	Ni	Cr	O	Fe
<i>Pristine Inconel 625</i>	61.73	25.15	-	4.13
<i>Polarized at $-0.3V$</i>	53.12	21.21	22.08	3.59

3 Contribution to Project Specific Objectives

The reported results make a contribution to the specific objective #1 (SO1): *Develop high-performance, cost-effective, and durable materials for direct seawater AEMWE components.*

The activities reported in this deliverable report directly address the topic of the durability of potential BPP and PTL materials that could be implemented in the direct seawater electrolyzer prototype. This contribution will be completed by the development and durability testing of innovative coatings in WT5.2, 5.3, and 5.4.

4 Contribution to major project exploitable result

As such and in view of the experimental results showing that most of the metals and alloys degrade under direct seawater electrolysis-mimicking conditions, the present deliverable does not contribute *directly* to a major exploitable result of the project. The main conclusion is that metallic elements, such as BPP or PTL, must be carefully selected and protected to be durable when implemented in the electrolyzer prototype. However, as planned in the work programme of the project, this deliverable provides a foundation for the next steps of the research activities, notably those dedicated to the development of novel protective coatings with an optimized trade-off between cost, sustainability, and durability of substrates (BPP, PTL) and coatings (WT5.2, WT 5.3, and WT5.4). The main exploitation perspectives are foreseen when combining the results of this deliverable (uncoated substrates) with the results of the BPP and PTL materials protected by the upcoming coatings.



5 Conclusions and Recommendations

This study shows that, in most cases, the metal and alloys in KOH solution (used in freshwater AEM electrolysis) in the absence of chlorides are stable. For instance, under such conditions, Ni is a suitable material. However, in the presence of chlorides (with a concentration of 0.6 M), most of the tested materials corrode under anodic conditions and therefore require a protective coating. Under cathodic conditions, the corrosion conditions are less severe (though still existing). The corrosion behavior of the different metals and alloys is summarized in Table 17.

Table 18: Summary of both anodic and cathodic polarization reactions at 50 °C in 1M KOH and ASW

	Anodic Polarization (1.6V to 2.2V; 50 °C; 1hr - 7days)		Cathodic Polarization (-0.3V to -0.2V; 50 °C; 2 - 7days)
	In 1M KOH	In alkaline ASW	In alkaline ASW
Ni	Stable	Pitting corrosion	-
Ti	Metal dissolution + Oxide/hydroxide layer formation	Pitting corrosion + oxide layer formation**	Oxide/hydroxide layer formation
316L	Metal leaching	Pitting corrosion*	Stable
Monel 400	Stable (short-duration results only: 3 hours, not shown in the report)	Pitting corrosion*	Stable
Inconel 600	Stable	Pitting corrosion	Stable
Inconel 625	Stable or Oxide/hydroxide Layer formation (depending on the applied potential)	Oxide/hydroxide layer formation	Stable
C22	Stable	Oxide/hydroxide layer formation***	-

* Crevice corrosion was observed at the (peripheral) gasket area.

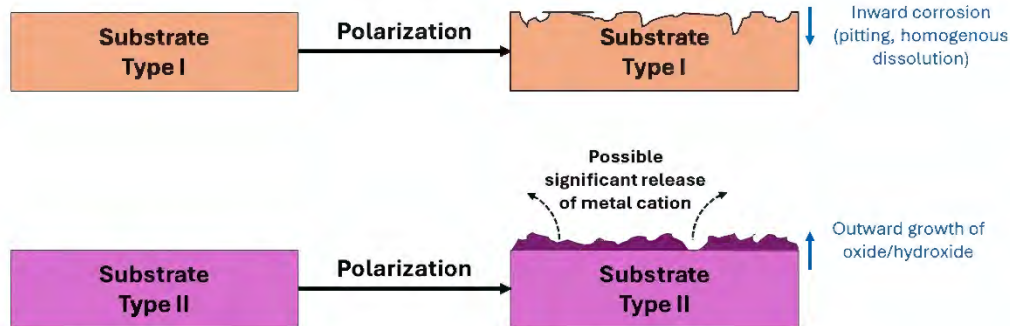
** Large increase of ICR ($>> 10 \text{ m}\Omega \cdot \text{cm}^2$) after polarization.

It is possible to distinguish two classes of substrates depending on how they degrade, as schematically depicted in Figure 23:

- Type I substrates exhibit the most severe degradation, such as pitting and homogeneous dissolution of the metals/alloys, with damages ranging from several tens of micrometers of depth to several millimeters (for long-duration testing), leading to perforation of the substrates. The direction of the degradation is “inward” (towards the bulk of the substrate). When a coating is applied to such substrates, the (almost unavoidable) defects of the coatings (e.g., pinholes) allow the aggressive agents of the electrolyte (such as chlorides) to attack the surface of the substrate below the coating and to form “blisters” that detach the protective layer and eventually rupture it. This has already been observed in the field of the PEM water electrolysis project “PROTIS” (coordinated by the French Corrosion Institute), as shown in Figure

23 for the case of 316L substrates. Developing durable coatings (at least, in thin-film form) for Type I substrate is quite challenging. In the SWEETHY project, Ni, Ti, 316L, Monel 400, and Inconel 600 can be considered as Type I substrates under anodic conditions.

(a) Uncoated Substrates



(b) Coated Substrates

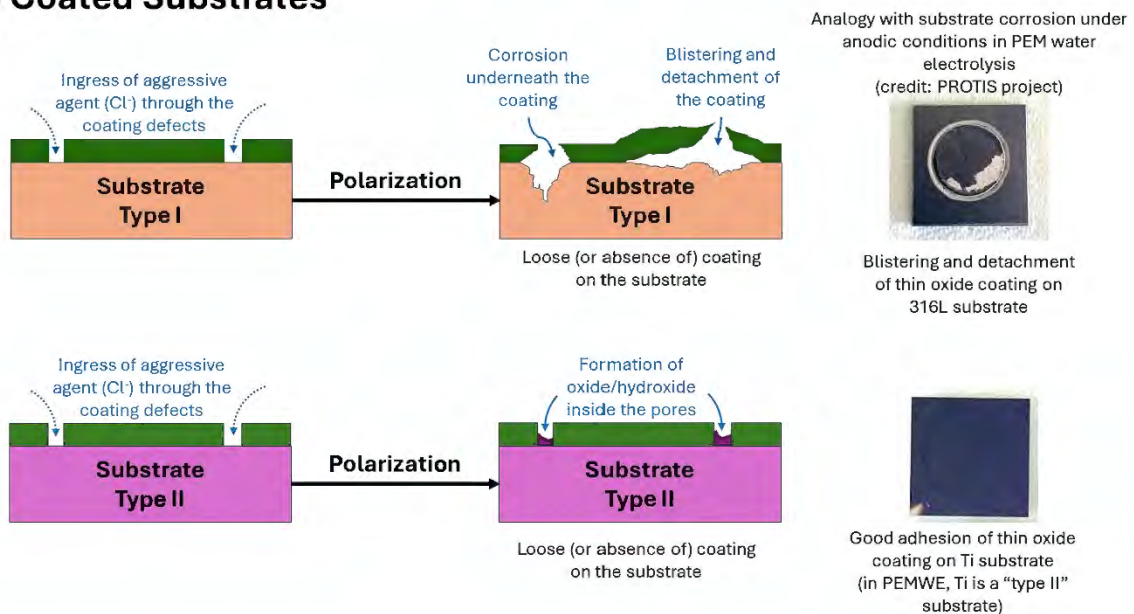


Figure 23: (a) Sketch of the two types of degradation of uncoated substrates in the present study and (b) their possible consequences on the durability of a subsequently applied coating.

- Type II substrates develop an oxide/hydroxide layer, whose direction of growth is “outward”. In general, oxide/hydroxide layers build up by dissolution of the outermost layer of the metal/alloys that reacts, very close to its surface, with the electrolyte to redeposit in the form of a more or less porous film that can be more or less protective. The thickness of the layers increases (to a certain level) with increasing applied potential, duration, and can be enhanced by the presence of chlorides. In the present study, molybdenum-containing alloys with a high content of chromium, namely Inconel 625 and C22, can be considered as Type II substrates under anodic conditions. When a coating is deposited onto such substrates, the non-protected areas (from defect coatings) are likely to undergo oxidation/hydroxylation, which would probably not affect the adherence of the coating (in contrast to a Type I substrate). It could also have a self-healing effect by clogging the coating defect. Hence, for the continuation of the



SWEETHY project, it is recommended to apply the coatings developed in WT5.2 on such Type II substrates as a priority.

The recommendation described above mainly concerns protection based on thin films (such as those produced by physical vapor deposition (PVD), chemical vapor deposition (CVD), electrodeposition, etc.) that contain defects giving aggressive species (such as chlorides) relatively easy access to the underlying metallic substrate. It might be that, when a thick-film approach is followed (e.g., by using plasma-spray techniques), this recommendation might differ, and that substrates of Type I may also be considered.



6 Acknowledgement

The author(s) would like to thank the partners in the project for their valuable comments on previous drafts and for performing the review.

Project partners:

#	Partner short name	Partner Full Name
1	RISE	RISE RESEARCH INSTITUTES OF SWEDEN AB
2	CNR	CONSIGLIO NAZIONALE DELLE RICERCHE
3	CIDETEC	FUNDACION CIDETEC
4	DLR	DEUTSCHES ZENTRUM FUR LUFT- UND RAUMFAHRT EV
5	IC	INSTITUT DE LA CORROSION SASU
6	SINTEF	SINTEF AS
7	PROPULS	PROPULS GMBH
8	CENMAT	CUTTING-EDGE NANOMATERIALS CENMAT UG HAFTUNGSBESCHRANKT
9	UNR	UNIRESEARCH BV

Disclaimer/ Acknowledgment

Copyright © – All rights reserved.

This document, or any part thereof, may not be published, disclosed, copied, reproduced, or used in any form or by any means without prior written permission from the SWEETHY Consortium. Neither the SWEETHY Consortium nor any of its members, their officers, employees, or agents shall be liable or responsible, whether in negligence or otherwise, for any loss, damage, or expense incurred by any person as a result of the use, in any manner or form, of any knowledge, information, or data contained in this document, or due to any inaccuracy, omission, or error therein.

All intellectual property rights, know-how, and information provided by or arising from this document—such as designs, documentation, and related preparatory material—are and shall remain the exclusive property of the SWEETHY Consortium and/or its members or licensors. Nothing in this document shall be interpreted as granting any right, title, ownership, interest, license, or any other rights in or to any such intellectual property, know-how, or information.

The project is supported by the Clean Hydrogen Partnership and its members.

Co-funded by the European Union under Grant Agreement No. 101192342. The views and opinions expressed are those of the author(s) only and do not necessarily reflect those of the European Union or the Clean Hydrogen Partnership. Neither the European Union nor the granting authority can be held responsible for them.

